RESEARCH ARTICLE

Analysis of spatiotemporal landscape patterns in ecological environment management

Jingyi Wang[1, *], Yan Song[2], Haozhong Yang[1], Minglan Zhou[3]

[1]School of Architecture, Xi'an University of Architecture & Technology, Xi'an, Shaanxi, China. [2]Survey Institute of Shaanxi Land Engineering Construction Group, Xi'an, Shaanxi, China. [3]College of Arts, Lanzhou University of Finance and Economics, Lanzhou, Gansu, China.

Received: January 20, 2025; **accepted:** June 10, 2025.

The spatiotemporal development of landscape patterns is the most obvious indicator of changes in land use and land cover and has significant implications for managing land use and optimizing regional landscape patterns. This research used middle reaches of the Yellow River in Shaanxi, China to construct the land use dataset based on thematic mapper (TM), enhanced thematic mapper plus (ETM+), and operational land imager (OLI) remote sensing images of 2014, 2017, 2020, and 2023 to construct a multi-layer perceptron network based on spatio temporal landscape ecological random forest (MLP-STLERF) to capture land use and land cover changes over time. The results showed that the area of cultivated land, urban land, other construction land, and rural residential land increased between 2014 and 2024, while the area of water, forest land, and grassland decreased during the previous ten years. Land use/land cover (LULC) was changed dramatically because of human activity, while landscape patterns and the eco-environment were also impacted. By combining the elements of each management zone's various ecological risk levels, the core zone, buffer zone, and experimental zone were defined to represent the ecological risk ranging from low to high. From 1986 to 2008, the ecological risk tended to be concentrated in one area, while, from 2014 to 2024, it marginally increased. The primary landscape types in Shaanxi were landscape level, forest land, green land, water land cultivated land, urban land, rural residential land, and unused land, which made up over 94% of the total area. Arable land and unused land were trending downward, while grassland and forest land were trending upward, and the percentage of construction land increased over the past ten years due to the rapid economic development. When compared to other current models, MLP-STLERF showed the best accuracy of 90.8% with a maximum accuracy of 98.2%. The proposed method outperformed root mean squared error (RMSE) in terms of minimizing absolute errors, while mean absolute error (MAE) was highly effective in explaining the spatial variations in landscape pattern change. The study offered a reference for optimizing landscape patterns in comparable geomorphic environments and allowed for a dynamic knowledge of the evolution of landscape patterns in typical hilly areas of northwest China.

Keywords: spatiotemporal; landscape pattern; ecological environment; land used; land change.

[*]**Corresponding author:** Jingyi Wang, School of Architecture, Xi'an University of Architecture & Technology, Xi'an 710055, Shaanxi, China. Email: jywong016@163.com.

Introduction

Land gives species the food and energy they need, and managing it is essential to preserving the environment and enhancing the quality of life. One of the most significant elements influencing ecosystem services and human well-being globally is the development of landscape patterns brought by land use and land cover changes (LULCs). The natural environment is under a lot of strain due to high-intensity land use and quick land-use changes by global socioeconomic growth [1]. Since ecological catastrophe and natural disasters brought on by the irresponsible use of natural resources directly affect national security, sustainable development, economic competitiveness, and regional landscape patterns, governments throughout the world have placed a great deal of emphasis on achieving ecological security [2]. The study of landscape units' type composition, spatial arrangement, and interactions with ecological processes is the focus of the broad field of landscape ecology. In addition to offering theoretical support and helpful advice for resolving several ecological and environmental issues that people confront, it aims to comprehend the stability and variety of ecosystems, biodiversity protection, land use planning, resource management, and ecological restoration [3].

The study of landscape patterns provides a tangible representation of landscape variation. The study demonstrated that human activity had an impact on aspect development and changes in addition to being directly linked to ecological processes such as soil nutrients, soil erosion, biodiversity, and soil moisture [4]. Landscape index analysis is one of the most popular techniques for analyzing landscape patterns. ML technology has been used in landscape pattern study, and geospatial information technologies like GIS and RS have become standard procedure used to obtain spatial data on landscape metrics [5]. A previous study examined spatiotemporal variations in landscape pattern and structure in the Greater Bay Area, China using remote sensing data from 1980 to 2020 and found the landscape pattern indices and the cities in that area having significant variations and diversities. However, the diffusion and coalescence processes in each city followed distinct patterns, and the landscape pattern and structural complexity increased gradually due to anthropogenic modifications [6]. To build and maximize the landscape pattern, Li *et al*. proposed a novel approach to assess the ecological hazards using the minimal cumulative resistance model (SPCA-RDA) and found that integrated ecological risk was greatly influenced by human social and landscape pattern variables with a low overall risk zone [7]. Previous research suggested that the ecological risk of the landscape was manageable, although the amount of agricultural land was declining and the amount of development land was growing. The study recommended building ecological shelters and making the most of available land [8]. Another study assessed landscape ecological risk (LER) and ecosystem service value (ESV) in China between 2000 and 2015 and found a rise in ESV and a fall in the LER index with plain regions primarily exhibiting high-LER, which affected sustainable development and ecological security [9]. An increase in vegetation area and fragment percentage was reported in a forest fragments analysis in a southern Brazil conservation unit from 1998 to 2018, while the edge density stayed low, suggesting less conservation. The results were essential for management plans and further study [10]. Wang *et al*. reported significant changes in land use and land cover by assessing landscape ecological risk from 1986 to 2015 [11], while Yan *et al*. looked at landscape ecological risk in the Three Gorges Reservoir Area from 1990 to 2020 and found that there had been a tendency toward more forest and building area and less agricultural land with precipitation, yearly average temperature, population density, and human influence as the primary motivators [12]. Abolmaali *et al*. investigated the connection between landscape patterns and habitat quality (HQ) in the watershed area surrounding Zayanderud Dam and discovered a downward trend in HQ with lower-quality habitats observed. The study emphasized how biodiversity was affected by landscape patterns and affected and supported efficient conservation and landscape management decision-making [13]. Understanding the level of ecological risks (ERs) may enhance sustainable development and the ecological environment. Scale transition was sensitive and looked at ER levels. Li *et al*. found that land-use intensity and degree were the primary barriers, whereas altitude and slope showed negative associations with ER [14]. The Chinese government has developed several conservation programs to address the conflict between human survival and development and the preservation of the environment and ecology in nature reserves [15]. Wang *et al*. reported that ecological restoration improved the ecosystem's worth, and conservation efforts and the creation of nature reserve networks might both support the enhancement of regional ecosystems [16].

To understand the effects of LULCs, a quantitative analysis of the changes in landscape patterns and the factors that influence them is thought to be essential. The significance of spatiotemporal scales is being emphasized more and more in research on the evolution of landscape patterns. Global, national, provincial, county, and township scales are among the administrative scales that have been the primary focus of research in recent years [17]. However, a few studies choose to employ landscape categories as the research boundaries including grasslands, wetlands, agricultural regions, and watersheds. Additionally, the pertinent quantitative research methodologies have expanded. Numerous studies have been conducted on land use prediction models, landscape metrics, geographical correlation, and the use of land suitability evaluation methods [18]. The analysis of landscape patterns' diversity, vulnerability, and structure has been the focus of research, and some studies have examined the causes and potential future changes in landscape pattern evolution using socioeconomic and natural factors like population, industry, vegetation, and terrain [19]. LULC change-based landscape machine learning approach is currently being used extensively to assess the effects of several risk variables in a region in a comprehensive manner and define how human disturbance or natural changes affect the landscape constitutions, structures, functions, and processes of a particular region [20]. This approach examined the impact of ecological hazards on the region's entire landscape in addition to the degree of damage to specific risk receptors. By combining geographical and ecological processes, the multi-layer perceptron (MLP) approach gives more consideration to the temporal and spatial variability of ecological hazards within a given area. The use of geographic information systems (GIS), remote sensing (RS), and multitemporal products can provide important information on landscape fragmentation mechanisms.

This research proposed a novel multi-layer perceptron network based on spatio temporal landscape ecological random forest (MLP-STLERF) model using GIS, RS, and multitemporal products to uncover localized spatial clustering of ecological risk in Shaanxi, China by quantifying the spatio-temporal changes in LULC and analyzing landscape patterns from 2014 to 2024 and highlighted how urban-rural transitional zones having evolved into new ecological risk hotspots, providing actionable insights for spatially targeted land-use planning and conservation policy. This study improved knowledge of the local ecological situation and measures, enhanced the accuracy of ecological landscape patterns, and created an integrated ecological pressure index. The results of this research would improve the precision of future forecasts and LULC change detection, facilitate in identifying environmental hazards and degradation trends by analyzing the effects of LULC changes on biodiversity, water resources, soil quality, carbon storage, and offer suggestions for sustainable land use planning, conservation tactics, and urban development by tying LULC findings to policy consequences.

Materials and methods

Study location and data sources

Located in the middle reaches of the Yellow River, Shaanxi is one of the most economically active and densely populated areas of northwest China with a very fragile ecological environment and significant soil erosion. With a total area of around 20.56 × 104 km^2, Shaanxi is also the location of the biggest and most characteristic

Loess Plateau in the world [21]. The terrain is high in the north and south and flat in the center. It is made up of a variety of geographical types including plains, mountains, plateaus, and basins, while the Loess Plateau makes up about 40% of the entire area. The region straddles the Yangtze and Yellow Rivers, has three distinct climate zones and 61 forest nature reserves, accounting for 5.6% of the total area, covering an area of 11.46×10^4 km². The area has numerous ecological reserves including wind and sand fixation, soil and water conservation, and is the primary area for the ecological protection project in the Yellow River Basin and the Three-North Shelterbelt Program [22]. The study areas were divided into experimental zone primarily where the highest and most dangerous risks were found, the buffer zone with the biggest reduction in ecological risk, and the core zone covered by the lowest and lowest danger. The data of administrative boundary, land use in 2014, 2018, 2020, 2024 with 30 m resolution, and digital elevation model (DEM) with Shuttle Radar Topography Mission (SRTM) digital elevation data in Geospatial Raster Data (GRID) format with 30 m resolution were acquired from China Land Use/Cover Dataset (CLCD) (China Academy of Sciences) (https://www.resdc.cn/).

Data preprocessing

Land sat Thematic Mapper (TM), Enhanced Thematic Mapper Plus (ETM+), and Operational Linescan System (OLS) remote sensing images were used to generate the land use dataset. When paired with an interpretation approach of human-computer interaction, the classification accuracy was confirmed in the field to be greater than 90.3%. The land use data was separated into 25 second-level land classes and six first-level land classes based on the use and natural characteristics of the land resources. The marshes were designated as wetland/water bodies in accordance with the requirements of the habitat quality research, whereas the other sandy land, Gobi, saline-alkali land, bare land, and bare rock land were designated as unused land. The spatiotemporal variation features of the ecological risk analysis of landscape patterns were analyzed. The object-oriented technique in eCognition 9.0 (https://geospatial.trimble.com/en/products/software/trimble-ecognition) was used to classify LULC from 1985 to 2015 using a random forest classifier. The ecological risk of the landscape was then assessed, and the features of its temporal and spatial change were examined. Multi-Layer Perceptron (MLP) and local spatial autocorrelation analysis using the Spatio temporal landscape ecological Random Forest (RF) approach were used to assess the ecological index's spatiotemporal aspects. Six LULC types were identified based on the actual conditions of the research region and the classification scheme designed for 30 m Landsat TM and ETM+ data including forest, cultivated land, grassland, alpine shrub land, built-up land, and water body. According to this categorization scheme, the built-up land contained highways and villages, while forest included coniferous, shrub, broad-leaved, and mixed broadleaf-conifer forests. The data from the forest resource inventory and Google Earth photos were used to choose the training and validation samples. The same training and validation samples were utilized in several time periods to guarantee the comparability of LULC classification findings. All samples remained constant between 2014 and 2024. The LULC changes from 2014 to 2024 were then analyzed using the MLP-STLERF algorithm by creating a land use transfer matrix using ArcGIS (https://www.arcgis.com/index.html).

MLP-STLERF algorithm

(1) Multi-layer perceptron network (MLP)

The first processing components of MLP were put up in a one-way approach. In these networks, three types of matching layers including the input, hidden, and output layers interacted with each other to produce new information. The sensor network that linked these landscape layers had several weighting values that fluctuated between [-1, 1]. Each node in an MLP was subjected to one of two function types of summation or activation. The product of the input values, weight values, and bias values were obtained using the summing function as follows.

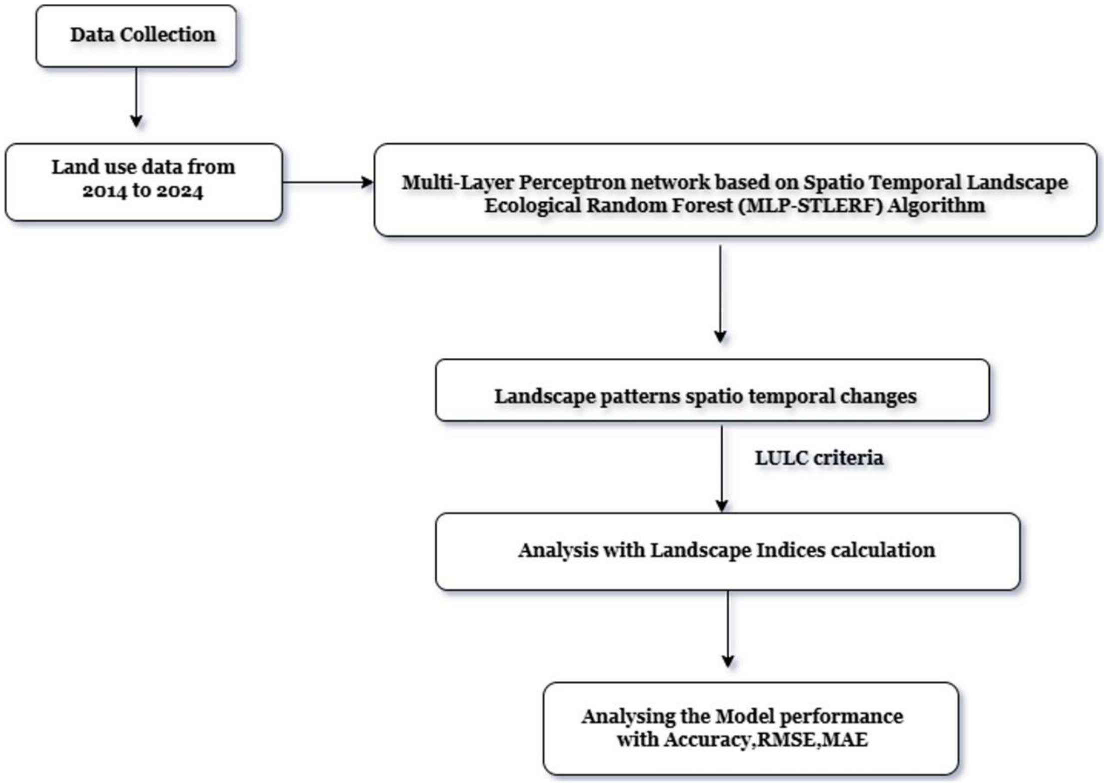

Figure 1. Flowchart of proposed MLP-STLERF algorithm.

$$T_i = \sum_{j=1}^{m} \omega_{ji} J_j + \beta_i \quad (1)$$

where ω_{ji} was the connection weight. β_i was a bias value. J_j was an input variable j. m was the total quantity of inputs. An activation function in line was then activated. Although there were other ways to activate the MLP, the S-shaped sigmoid function was the most widely used one and was calculated as below.

$$e_i(w) = \frac{1}{1+e^{-T_i}} \quad (2)$$

Equation (3) was then used to determine the neuron i's ultimate output.

$$z_j = e_j\left(\sum_{j=1}^{m} \omega_{ji} J_j + \beta_i\right) \quad (3)$$

Learning started after the final structure of the RF was built to refine and evolve the weighting vectors of the network. These weighting vectors needed to be adjusted to estimate the results and maximize the network's overall error. The Random Forest's computationally demanding training phase significantly affected the MLP's efficacy and problem-solving skills. The workflow of the proposed method was shown in Figure 1.

(2) Spatio temporal landscape ecological random forest (STLERF)

To improve the system's classification accuracy, the decision tree node division technique employed an adaptive parameter selection strategy. Selecting different node-splitting algorithms for the same data set also resulted in different decision trees, even when the attributes varied. Since the accuracy of RF classification varied, a decision tree was used to select the best feature for dividing the nodes to develop a new splitting rule that was used for selecting and splitting node characteristics. There were two categories for the node splitting technique including linear combination. The Gini index and the information gain that was achieved when the sample set C was divided using features were displayed, employing the node splitting formula 4 and 5 below.

$$Gain(C,b) = Ent(C) - \sum_{u=1}^{U} \frac{|C^u|}{|C|} Ent(C^u) \quad (4)$$

$$Gini(C,b) = \sum_{u=1}^{U} \frac{|C^u|}{|C|} Gini(C^u) \quad (5)$$

where C^u was that every sample in the C with a value of b^u on a feature b was found in the u branch node.

$$Ent(C) = -\sum_{l=1}^{|z|} o_l log_2 o_l \quad (6)$$

$$Gini(C) = \sum_{l=1}^{|z|} \sum_{l' \neq l}^{|Z|} olol' = 1 - \sum_{l=1}^{|z|} ol^2 \quad (7)$$

The adaptive parameter selection procedure and combination node splitting formula were as follows to attempt an increased purity of the data set after splitting.

$$G = \min_{\alpha, \beta \in Q} E\{C,b\} = \alpha Gini(C,b) - \beta Gain(C,a)$$

$$s.t. \begin{cases} \alpha + \beta = 1 \\ 0 \leq \alpha, \beta, \leq 1 \end{cases} \quad (8)$$

where α, β were the characteristic's splitting weight coefficient. Meantime, G had a very low value. The procedure of adaptive parameter choice was utilized to obtain the ideal combination of parameters. The accuracy rate and categorization error rate were utilized in the study to evaluate efficiency. The sample C categorization error rate was defined as follows.

$$F(e;C) = \frac{1}{n} \sum_{j=1}^{n} \mathrm{II}\left(e\left(w_j\right) \neq z_j\right) \quad (9)$$

The accuracy percentage was defined as below.

$$acc(e;C) \frac{1}{n} \sum_{j=1}^{n} II\left(e\left(w_j\right) = z_j\right) = 1 - 1F(e;C) \quad (10)$$

Comparison of proposed method with other exist methods

To evaluate spatio temporal landscape patterns for the ecological risk based on proposed machine learning algorithm (MLP-STLERF), the accuracy of proposed algorithm was compared to the existing methods including CNN-LSTM [23] and Moran's Value [24].

Results and discussion

Changes in land use

Shaanxi province's primary land use categories in 2010 were forest land (38.01%) and agricultural land (42.88%). Only 1.18%, 8.13%, 6.20%, and 0.97% of the entire research region was made up of grassland, water area, rural residential land, and urban land, respectively. There was little urbanization, and the study region was mostly composed of forests and agriculture. Significant changes in land use were seen in 2019. The areas of forest land, grassland, and water area dropped by 5.4%, 18.19%, 2.18%, while urban land, other construction land, and rural residential land grew by 33.26%, 21.22%, 19.42%, respectively (Figure 2). While forest land, grassland, and water areas all declined during the last ten years, development land area increased significantly.

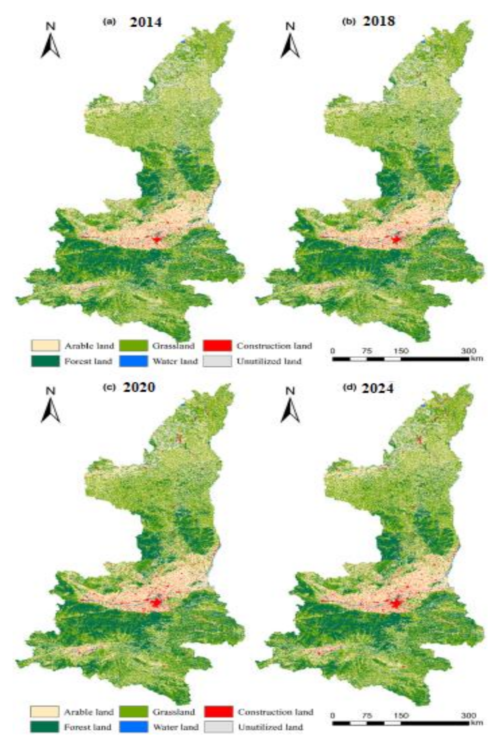

Figure 2. Land used categories for past 10 years.

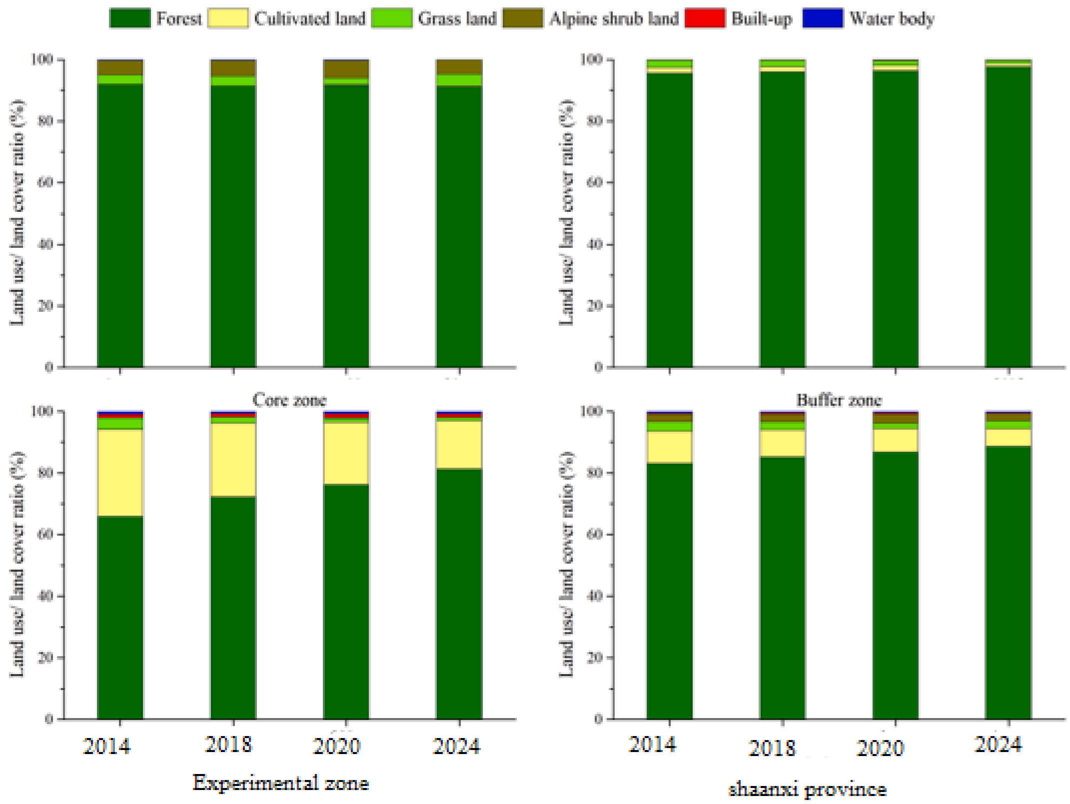

Figure 3. Various LULC types in the core zone, buffer zone, experimental zone, and the whole reserve.

Features of land use and land cover changes throughout time and space

The LULC spatial distribution maps created with MLP-STLERF between 2014 and 2024 demonstrated that the most prevalent LULC type was forest. Cultivated terrain was mainly found in level valleys with plenty of water and rich soil. Grasslands were dispersed across the reserve. Due to height constraints, alpine shrub land was dispersed over the highland area and developed in areas with convenient water supplies and agricultural development. Between 2014 and 2024, the total area of forest expanded by 100.88 km². Additionally, the cultivated land area shrank by 85.23 km². The 87.46 km^2 of farmed land that made up most of the expanded forest area was transferred. There were no discernible change trends in the built-up area, water body, alpine shrub land, or grass land. The results further displayed the area ratios of the various LULC types in the core zone, buffer zone, experimental zone, and the whole reserve in 2014, 2018, 2020, and 2024. Forest, cultivated land, grass land, alpine shrub land, built-up, and water body were the LULC types with the highest and lowest area ratios to the total area of the whole reserve. Over 83% of the land was covered by forests, and between 2014 and 2024, this percentage increased from 83.12% in 2014 to 88.54% in 2024. The proportion of cultivated land to total area fell from 10.42% in 2014 to 5.84% in 2024, indicating a declining trend in the area under cultivation. Between 2014 and 2024, the area ratios of the other LULC classes remained mostly constant. The LULC types in the core zone were alpine shrub land, grassland, and woodland. More than 85% of the core zone was made up of forest, which was the predominant type. Because of the elevation restriction, alpine shrub land was only found in the core zone. Out of the three management zones, the buffer zone had the lowest area with LULC categories as grassland, cultivated land, and woodland. The forest's percentage was over 95% and was trending upward from 2020. The growing forest was moved from grassland and agricultural areas. Over the course of ten years, the percentage of forest in the experimental zone went from 65.81% to 81.22% with an increase of 102.61 km². The ratio of farmed land fell from 28.33% to 15.74% with a declining area of 83.56 km^2. A total of 85.60 km^2 of farmed land was turned over to the forest. Grass land covered 2.70 km^2 with a little bit decline. Water bodies and built-up areas were mostly found in the experimental zone, and their modifications were barely noticeable. Following an accuracy evaluation, the total LULC classification accuracies from 2014 to 2024 was 86.36%, 85.51%, 85.69%, and 85.72%, respectively (Figure 3). These results might be used to fulfill the needs of landscape research in general.

The structural dynamics of the landscape type might be more accurately described at the class level by examining a collection of landscape indices. Different terrain types had shown variations in their patterns throughout the last ten years. The biggest patch index and the percentage of landscape index for agricultural land showed a general decreasing trend, suggesting a decline in both the amount of agricultural land and the landscape advantage. The growth of agricultural land was towards a complex form and geographical fragmentation was represented in the rise in the landscape shape index and the fall in the aggregation index. While the patch density index and landscape form index showed a declining trend, the proportion of the landscape index grew for forests, suggesting that the patches' growing shapes tended to be smooth. The reducing public border was the main cause of the higher aggregation index, whereas the nearby patches displayed linked patch-like development. As the proportion of landscape index climbed in the case of building land, the patch density index, edge density index, and landscape form index all increased (Figure 4). The results suggested that the extension of the construction land area was mostly dependent on the growth of the number of patches, which filled in the spaces between them, improving their connectedness and raising the construction land's aggregation index.

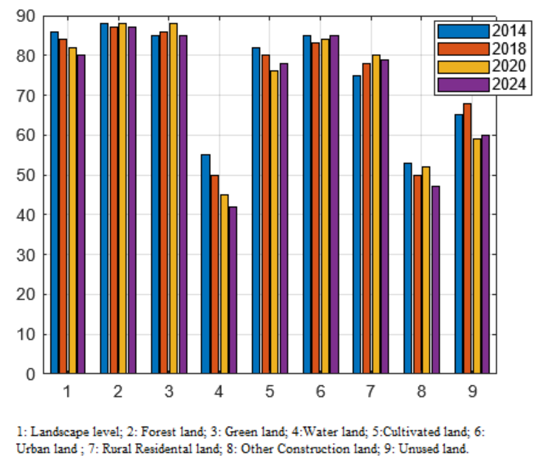

Figure 4. Overall Landscape combined with different index.

Accuracy comparison of proposed model with other existing models

The classification accuracies of proposed MLP-STLERF model, the CNN-LSTM model, and Moran's value-based approach were 90.8%, 80.2%, and 88.6%, respectively (Figure 5), which suggested that the MLP-STLERF model provided better accuracy in identifying ecological dynamics and spatiotemporal patterns of land use. The model's ability to better grasp intricate spatial relationships and temporal fluctuations was due to its combination of deep learning with landscape ecology concepts, which was responsible for its improved performance.

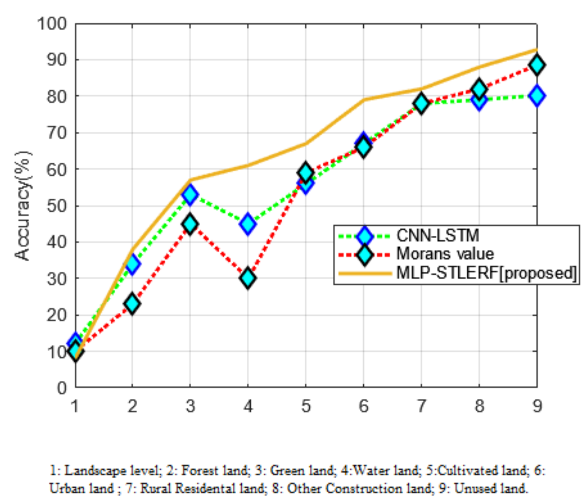

Figure 5. Outcome of accuracies of compared models.

The mean absolute error (MAE) offered a simple way to evaluate the range of the mistake by counting the regular absolute disparities among the observed and predictable values of ecological location. Since MAE switched all mistakes equally, it was less susceptible to outliers than root mean square error (RMSE) and could be useful in some conditions. The MAE of proposed MLP-STLERF model was 0.01, which validated its superiority in capturing real values, while the values of MAE for Moran and CNN-LSTM were 0.08 and 0.11, respectively, indicating the improved performance of the proposed method in minimalizing absolute errors. RMSE is an indicator of how much forecasts differ from actual outcomes and is a commonly used metric that calculates the average greatness of errors between expected and observed values. To highlight bigger errors brought on by squaring, it squares the discrepancies among the foreseeable and actual values, medians them, and then calculates the square root. The results showed that the proposed MLP-STLERF model achieved a RMSE value of 0.015, which was a comparatively low prediction error compared to that of Moran's value of 0.12 and CNN-LSTM's value of 0.127, indicating that the proposed model was effective in reducing develop errors (Table 1).

Table 1. Numerical outcomes of RMSE and MAE.

Methods	RMSE	MAE
CNN-LSTM	0.127	0.11
Moran	0.120	0.08
MLP-STLERF	0.015	0.01

Spatial temporal landscape ecology is the most used technique for evaluating landscape patterns. When applied to LULC, random forest is appropriate for several scales and may achieve the spatiotemporal manifestations of multi-source risk with few *in situ* data. Nevertheless, there were several obvious ambiguities in the study including the heavy reliance on LULC results that the LULC inaccuracy might result in earned run average (ERA) uncertainty and LULC map errors that might reduce LULC data accuracy. Throughout 1986 to 2015, forests accounted for almost 80% of the total area, making them the predominant LULC category. As people pay more and more attention to environmental protection, the most important transfer features of LULC are the reduction of cultivated land and the growth of forest. While the LULC was comparatively steady in the core and buffer zones, the LULC transfer occurred most sensitively in the experimental zone with the total ecological risk dropped from 2020. Over the course of the ten years, the geographic aggregation of ecological risk steadily diminished with marginal improvement in 2020. The natural flora had been replaced by rubber forest and tea plantation regions, causing tropical rainforests to become much more fragmented. Landscape ecological risk is influenced by both environmental and social variables including temperature, precipitation, population density, and human involvement. These influences have complicated driving mechanisms and regional variability.

References

1. Wang H, Wang WJ, Wang L, Ma S, Liu Z, Zhang W, *et al*. 2022. Impacts of future climate and land use/cover changes on water-related ecosystem services in Changbai mountains, northeast China. Front Ecol Evol. 10:854497.
2. Wang LJ, Ma S, Zhao YG, Zhang JC. 2021. Ecological restoration projects did not increase the value of all ecosystem services in Northeast China. For Ecol Manag. 495:119340.
3. Xu S, Li S, Zhong J, Li C. 2020. Spatial scale effects of the variable relationships between landscape pattern and water quality: Example from an agricultural karst river basin, Southwestern China. Agric Ecosyst Environ. 300:106999.
4. Ren J, Yan D, Ma Y, Liu J, Su Z, Ding Y, *et al*. 2022. Combining phylogeography and landscape genetics reveals genetic variation and distribution patterns of *Stipa breviflora* populations. Flora. 293:152102.
5. Yu Z, Song D, Song Y, Lau SK, Han S. 2022. Research on a visual thermal landscape model of underground space based on the spatial interpolation method—A case study in Shanghai. Energy Rep. 8:406–418.
6. Abbas Z, Zhu Z, Zhao Y. 2022. Spatiotemporal analysis of landscape pattern and structure in the Greater Bay Area, China. Earth Sci Inform. 15(3):1977–1992.
7. Li S, He W, Wang L, Zhang Z, Chen X, Lei T, *et al*. 2023. Optimization of landscape pattern in China Luojiang Xiaoxi

basin based on landscape ecological risk assessment. Ecolo Indic. 146:109887.

8. Zeng C, He J, He Q, Mao Y, Yu B. 2022. Assessment of land use pattern and landscape ecological risk in the Chengdu-Chongqing economic circle, Southwestern China. Land. 11(5):659.
9. Bian J, Chen W, Zeng J. 2022. Ecosystem services, landscape pattern, and landscape ecological risk zoning in China. Environ Sci Pollut Res. 30(7):17709–17722.
10. Fernandes B, Batista L. 2020. Spatial-temporal analysis of the forest fragments surrounding a conservation unit in the southern region of Brazil. Environ Sci Proc. 3(1):48.
11. Wang H, Liu X, Zhao C, Chang Y, Liu Y, Zang F. 2021. Spatial-temporal pattern analysis of landscape ecological risk assessment based on land use/land cover change in Baishuijiang National nature reserve in Gansu Province, China. Ecolo Indic. 124:107454.
12. Yan Z, Wang Y, Wang Z, Zhang C, Wang Y, Li Y. 2023. Spatiotemporal analysis of landscape ecological risk and driving factors: A case study in the Three Gorges Reservoir area, China. Remote Sens. 15(19):4884.
13. Abolmaali SM, Tarkesh M, Mousavi SA, Karimzadeh H, Pourmanafi S, Fakheran S. 2024. Impacts of spatio-temporal change of landscape patterns on habitat quality across Zayanderud Dam watershed in central Iran. Sci Rep. 14(1):8780.
14. Li L, Zhou X, Yang L, Duan J, Zeng Z. 2022. Spatio-temporal characteristics and influencing factors of ecological risk in China's north–south transition zone. Sustainability. 14(9):5464.
15. Zhang H, Liang X, Chen H, Shi Q. 2021. Spatio-temporal evolution of the social-ecological landscape resilience and management zoning in the loess hill and gully region of China. Environ Develop. 39:100616.
16. Wang X, Zhang C, Wang C, Liu G, Wang H. 2021. GIS-based for prediction and prevention of environmental geological disaster susceptibility: From a perspective of sustainable development. Ecotoxicol Environ Saf. 226:112881.
17. Abdollahi S, Zeilabi E, Xu CCY. 2023. Habitat quality assessment based on local expert knowledge and landscape patterns for bird of prey species in Hamadan, Iran. Model Earth Syst Environ. 10(2):2051–2061.
18. Abdollahi S. 2024. Habitat quality assessment of wild life to identify key habitat patches using landscape ecology approach. J Nat Environ. 76(Special Issue):147–162.
19. Abolmaali SM, Tarkesh M, Mousavi SA, Karimzadeh H, Pourmanafi S, Fakheran S. 2024. Identifying priority areas for conservation: using ecosystem services hotspot mapping for land-use/land-cover planning in central of Iran. Environ Manag. 73(5):1016–1031.
20. Motlagh ZK, Lotfi A, Pourmanafi S, Ahmadizadeh S, Soffianian A. 2020. Spatial modeling of land-use change in a rapidly urbanizing landscape in central Iran: integration of remote sensing, CA-Markov, and landscape metrics. Agric Ecosyst Environ. 192(11):695.
21. Zhang SL, Gao PC, Tong YA, Norse D, Lu YL, Powlson D. 2015. Overcoming nitrogen fertilizer over-use through technical and advisory approaches: A case study from Shaanxi Province, northwest China. Agric Ecosyst Environ. 209:89–99.
22. Zhao ZP, Yan S, Liu F, Wang XY, Tong YA. 2014. Analysis of nitrogen inputs and soil nitrogen loading in different kinds of orchards in Shaanxi Province. Acta Ecologica Sinica. 34(19): 5642-5649.
23. Masolele RN, De SV, Herold M, Marcos D, Verbesselt J, Gieseke F, *et al*. 2021. Spatial and temporal deep learning methods for deriving land-use following deforestation: A pan-tropical case study using Landsat time series. Remote Sens Environ. 264:112600.
24. Zhang M, Ma S, Gong JW, Chu L, Wang LJ. 2023. A coupling effect of landscape patterns on the spatial and temporal distribution of water ecosystem services: A case study in the Jianghuai ecological economic zone, China. Ecol Indic. 151:110299.